JACS
JOURNAL OF THE AMERICAN CHEMICAL SOCIETY

ARTICLE

pubs.acs.org/JACS

Direct Imaging and Probing of the p−n Junction in a Planar Polymer Light-Emitting Electrochemical Cell

Yufeng Hu and Jun Gao*

Department of Physics, Engineering Physics, and Astronomy, Queen's University, Kingston, Ontario K7L 3N6, Canada

Supporting Information

ABSTRACT: A vast array of semiconductor applications relies on the ability to dope the materials by the controlled introduction of impurities in order to achieve desired charge carrier concentration and conduction type. In this way, various functional metal/semiconductor or semiconductor/semiconductor junctions can be constructed for device applications. Conjugated polymers are organic semiconductors that can be electrochemically doped to form a dynamic p−n junction. The electronic structure and even the existence of such a polymer p−n junction had been the subject of intense scrutiny and debate. In this work, the formation of the world's largest frozen polymer p−n junction and its light-emission are visualized. With a pair of micromanipulated probes, we mapped the potential distribution of the p−n junction under bias across the entire interelectrode gap of over 10 mm. Site-selective current−voltage measurements reveal that the polymer junction is a graded p−n junction, with a much more conductive p region than n region.

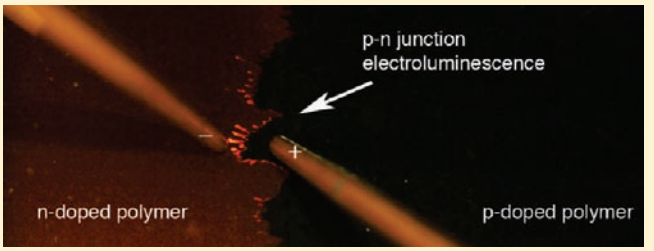

INTRODUCTION

Organic semiconductors, and particularly conjugated polymers, are attractive alternatives to conventional inorganic semiconductors for device applications due to their low cost and mechanical flexibility.[1] The field of organic electronics has seen rapid advancement over the past decade. Many conventional inorganic semiconductor devices now have organic counterparts; for instance, organic light-emitting diodes,[2] solar cells,[3−5] and field-effect transistors[6,7] have all been demonstrated with respective performance. Although organic semiconductors can be easily p- or n-doped to achieve higher conductivity,[8−13] the latest organic devices typically do not involve intentional doping to create a functional homojunction or ohmic contact except in a few cases.[14−18] A polymer light-emitting electrochemical cell (LEC) is a unique device whose active layer is a mixed ionic/electronic conductor consisting of a luminescent conjugated polymer and a solid-state polymer electrolyte.[19,20] An LEC after turn on is not only doped but also a p−n junction analogous to a conventional inorganic p−n junction.

A p−n junction is at the heart of many conventional semiconductor devices due to its unparalleled versatility as an injector of minority charge carriers, a separator of photogenerated charge carriers, a rectifier, or a variable resistor/capacitor.[21] Not surprisingly, an organic analog was attempted immediately following the discovery of conducting polymers by intentional chemical doping.[22,23] In parallel with inorganic semiconductors, chemical doping or ion implantation was employed in the early works to create an organic p−n junction with some success.[24−27] Unlike inorganic semiconductor doping, however, the dopant counterions do not form covalent bonding with the host molecules, leaving them somewhat mobile at room temperature. As a result, the chemically doped polymer p−n junction tends to relax by diffusion. This has led to the attempt to covalently bond the dopant counterions to the polymer backbone.[28] The LEC represents a unique approach to form an organic p−n junction. Doping in an LEC is achieved by applying a dc bias larger than E_g/e, where E_g is the energy gap of the semiconducting polymer and e the elementary charge. Under the applied bias, the semiconducting polymer is oxidized near the anode (positive electrode) and reduced near the cathode. At the same time the available counterions from the polymer electrolyte drift to the oxidized or reduced sites to maintain local charge neutrality. This constitutes in situ electrochemical p- and n-doping. The doped regions would grow in size until they meet to form a dynamic light-emitting p−n junction in between the electrodes. The p−n junction is called dynamic because it dissipates once the applied bias is removed. Various chemical approaches have been devised to permanently fix the LEC p−n junction by using polymerizable counterions and/or ion transport materials.[29−31] A physical and more simple way to stabilize the polymer p−n junction is to cool the LEC, once turned on, to a temperature below the glass transition temperature (T_g) of the polymer electrolyte used. This renders the electrolyte ions immobile, creating a frozen doping profile.[32−34]

A primary consequence of doping, like in inorganic semiconductors, is the dramatic increase in conductivity. This allows an LEC to operate in a planar configuration with an extremely large

Received: October 15, 2010
Published: January 28, 2011

   dx.doi.org/10.1021/ja1093106 | J. Am. Chem. Soc. 2011, 133, 2227–2231

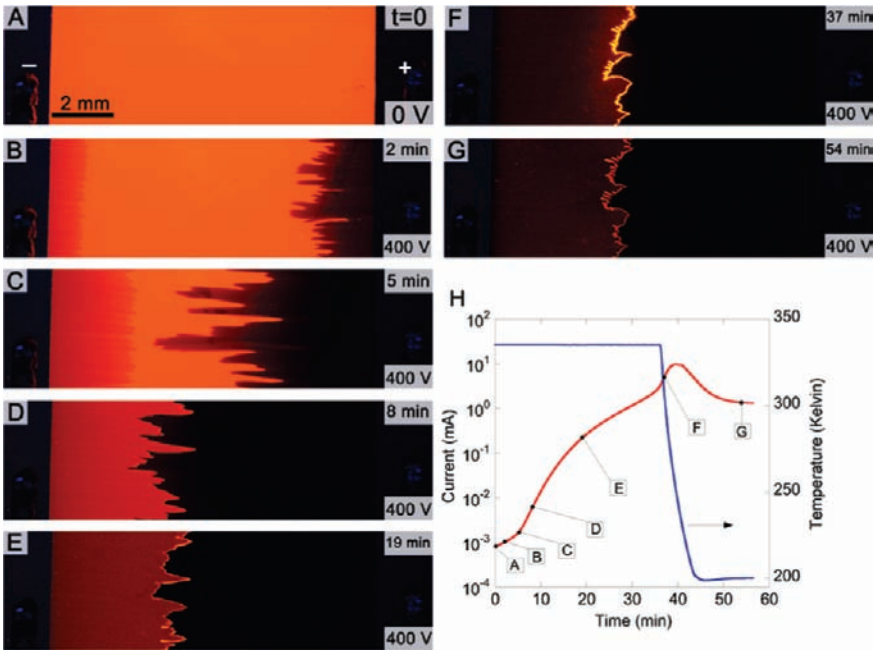

Figure 1. Time-lapse fluorescence imaging of a 10.4 mm MEH-PPV:PEO:$CsClO_4$ planar LEC during turn on and cooling. A fixed dc bias of 400 V was applied to turn on the cell, which was at 335 K and under UV illumination. Time since the dc bias was applied to the cell: (A) no bias, (B) 2 min, (C) 5 min, (D) 8 min, (E) 19 min, (F) 37 min, (G) 54 min. Panel H shows cell current and temperature as a function of time since the dc bias was applied. Uniform enhancement (level adjustment in Photoshop) has been applied to images A−G.

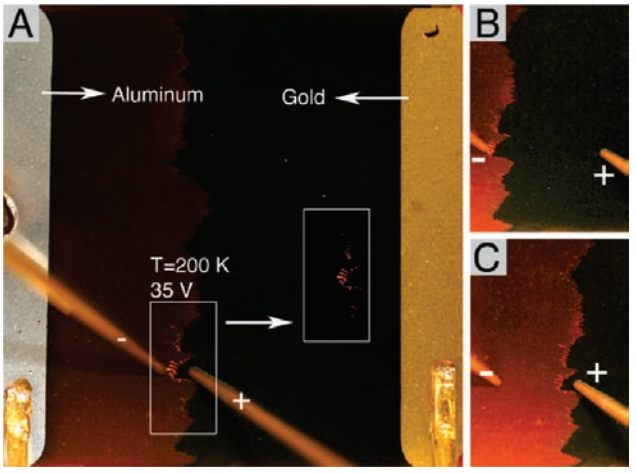

Figure 2. Imaging of electroluminescence in the same LEC as shown in Figure 1. The gold and aluminum electrodes were not biased. A 35 V bias was applied between the two gold-coated tungsten probes. Panel A gives a full view of the LEC with some room light filled in to review the electrodes. The box to the left shows the region with EL. The box to the right shows the same region imaged in dark. Panels B and C show the effect of moving positive (panel B) or negative (panel C) probe away from the junction. Uniform enhancement (level adjustment in Photoshop) has been applied to images B and C. Separate level adjustment has been applied to panel A.

interelectrode spacing.[35] The dynamic doping propagation and junction formation processes have been visualized via fluorescence imaging, providing a dramatic confirmation of the fundamental LEC operating mechanism.[36−39] The fully exposed surface of a planar LEC also allows electrical probing of potential or field distribution of a biased LEC. Scanning probe microscopic techniques have recently been applied to dynamic junctions of small (micrometer-scale interelectrode spacing) planar LECs under bias.[40,41] In this work, we present an unprecedented study of the world's largest frozen planar LECs using combined techniques of fluorescence imaging and contact probing in a cryogenic probe station.

RESULTS AND DISCUSSION

The 10.4 mm cells in this study had dissimilar electrodes (gold/aluminum) to facilitate hole/electron injection and thus doping initiation.[42] The cells also contained cesium salt rather than the commonly used lithium salt to realize a more centered junction position due to better matching of cation and anion size.[43,44] To turn on the planar LEC, a dc bias of 400 V was applied between the gold and aluminum electrodes, with gold wired as the positive electrode. The device was also heated to 335 K to increase ion mobility. This combination of operating temperature and turn-on voltage gave rise to a reasonably fast turn on process that can also be easily imaged, as shown in Figure 1. Under UV illumination, the polymer film displayed the characteristic orange-red photoluminescence (PL) of MEH-PPV (Figure 1A). The dc bias triggered electrochemical doping of MEH-PPV to initiate from the electrode interfaces and propagate toward the opposite electrodes (Figure 1B,C). Electrochemical doping is visible as it causes strong PL quenching in the film, so under UV illumination the doped regions appear darker than the intrinsic film. The darker p-doping expands at a faster rate than n-doping, leading to the formation of a continuous but jagged p−n junction closer to the cathode (Figure 1D). With time, electroluminescence (EL) became discernible along the p−n junction against the background PL (Figure 1E). It is important to note that the doping level continued to increase after junction formation, as evidenced by the darkening of the n-doped region, and that the EL intensity increased (Figure 1F). When the device current was well into the mA range, the device was cooled to

dx.doi.org/10.1021/ja1093106 |J. Am. Chem. Soc. 2011, 133, 2227–2231

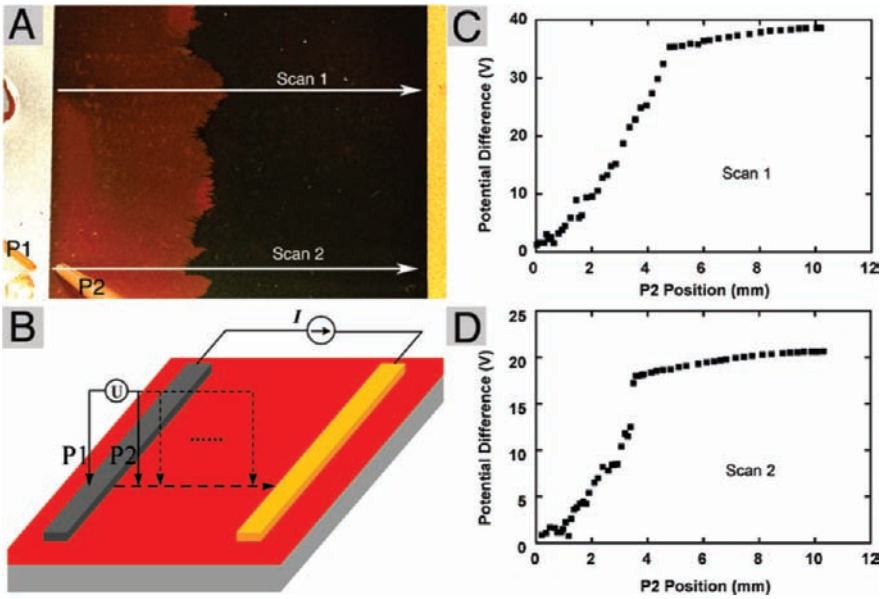

Figure 3. Potential mapping of the frozen-junction LEC shown in Figures 1 and 2. Panel A shows the location and the direction of the two scans conducted. Panel B shows the biasing conditions for both the LEC and the probes. Panel C shows the potential profile obtained in Scan 1 with an applied current of 50 μA and voltage of 38.65 V. Panel D shows the potential profile obtained in Scan 2 with an applied current of 25 μA and voltage of 20.65 V. Level adjustment has been applied to panel A in Photoshop.

200 K in about 9 min, with the 400 V bias maintained across the electrodes (Figure 1H). Even at 200 K, EL remained highly visible (Figure 1G) despite the greatly reduced current. The doping and p−n junction formation was accompanied by a sharp increase in device current despite a fixed bias (Figure 1H). Eventually, the current dropped in response to the temperature decrease. The current leveled off at about 1.3 mA at 200 K from the peak of almost 10 mA. The fixed 400 V bias was subsequently removed to allow various measurements on the frozen cell.

Although a large bias must be applied to turn on the extremely large LEC for the first time, a much lower bias was sufficient to induce observable junction EL when the vast bulk of the neutral doped p and n regions are bypassed. The stripe gold and aluminum electrodes were disconnected. And a pair of gold-coated tungsten probes was maneuvered into direct contact with the doped polymer film at close proximity (~0.7 mm) directly across the p−n junction. EL was imaged with only a 35 V bias between the probes and was confined to the junction region close to the probe tips (Figure 2A). The size of emission zone did not change when the positive probe (the probe in contact with the p-doped region) was moved away from the junction (Figure 2B). This suggests the p-doped polymer is a good (perhaps metallic) conductor with very little potential drop. By contrast, moving the negative probe away caused a much longer section of the junction to emit (Figure 2C). This observation suggests that the n-doped film was much less conductive.

Next, a constant forward current of 25 or 50 μA was applied to the frozen-junction LEC via the gold and aluminum electrodes. The potential distribution across the entire cell was mapped by fixing probe P1 to the aluminum electrode, while scanning the other probe (P2) along the two lines shown in Figure 3A. The potential difference between P1 and P2 was recorded with a Keithley 237 source measure unit by nulling the current between P1 and P2.

Both scan lines across the device (Figure 3C,D) showed a sharp transition in potential drop where the p−n junction was located. Most of the voltage drop was in the n region (~90%). This suggests the n region was much more resistive than the p region, confirming the observations shown in Figure 2. It is also noted that the potential distribution is not linear in either p or n regions. The potential profile is visibly more flat near the electrodes, implying higher conductivity and doping level. The potential profiles obtained above are similar to those measured by Matyba et al. in planar MEH-PPV:PEO:KCF_3SO_3 cells using scanning Kelvin probe microscopy (SKPM).[41] This is a remarkable agreement considering the different techniques used, operating conditions (dynamic junction at room temperature vs frozen junction at 200 K) and cells dimensions (120 μm vs 10.4 mm). SKPM measurements by Pingree et al. on 15 μm dynamic planar LECs observed that potential drop was mainly near the cathode interfaces.[12,40] This is most likely due to their use of lithium salt in their cells, which typically leads to a very off-centered emitting junction near the cathode. Indeed, by replacing the lithium salt with a potassium salt, the authors recently observed EL that was shifted away from the cathode. The potential profile of a planar cell with gold electrodes is qualitatively consistent with our results in that the potential drop mainly occurs in n-doped region and there is little potential drop near the electrodes.[45]

With our setup and a frozen cell it is possible to conduct current−voltage (I−V) scans at various locations to probe the local conductivity. For this study both tungsten probes are lowered to make direct contact with the polymer film. Contact was confirmed by monitoring the tip current under a fixed bias. For comparable probe spacing and bias voltage, the probe current is more than an order of magnitude higher in the p region than in the n region, as shown in Figure 4A,B. This provides the most direct evidence of high conductivity in the p region relative to the n region. In both regions the I−V curves display some curvature due to nonohmic contact between the probe and the doped film. To map the conductivity profile, the pair of probes was scanned together at a spacing of approximately

dx.doi.org/10.1021/ja1093106 |J. Am. Chem. Soc. 2011, 133, 2227–2231

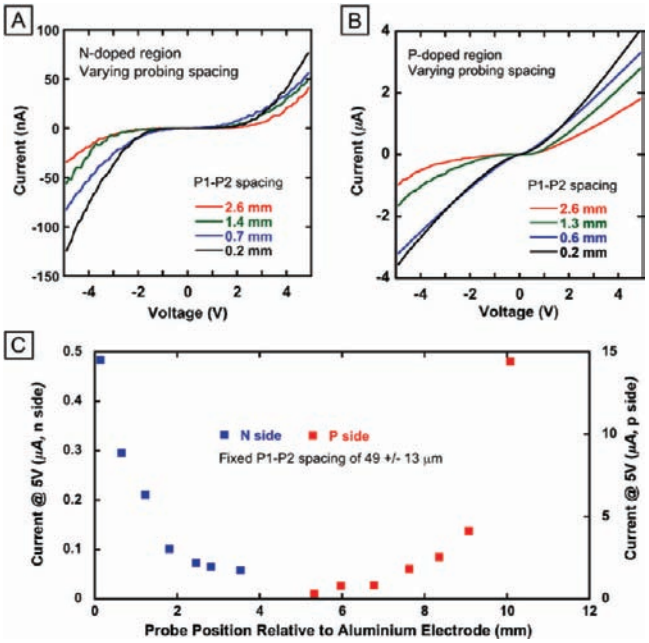

Figure 4. Current vs voltage probing of a separate 10.4 mm frozen-junction planar cell at 200 K similar to that shown in Figure 1. (A) n-Doped region with varying probe spacing. (B) p-Doped region with varying probe spacing. (C) Probe current at 5 V as a function of probe-to-aluminum electrode distance with the probe spacing fixed. The probes are made of tungsten. The line joining the two probe contacts is made to be perpendicular to the stripe electrodes.

50 μm across the entire interelectrode gap. Probe current at a fixed bias of 5 V was recorded and plotted as a function of probe location, as seen in Figure 4C. This current serves as a measure of the local conductivity. Again, the current in the p region is much higher than in the n region. Moreover, the data clearly shows that the film conductivity is the highest near the electrodes and decreases toward the junction. Hence, the frozen planar LEC is a graded p−n junction. The high conductivity of the polymer film near the electrodes suggests that the anode (or cathode)/polymer interface is likely an ohmic contact. This explains why there is negligible potential drop at the electrode interfaces in our devices (see Figure 3). The interfacial electrical field strength, on the other hand, should be high, although it cannot be measured with the current setup. By contrast, the observation of significant voltage drop near the electrode interfaces in some micrometer-scale planar cells might suggest insufficient or absence of doping.[45,46] We note that when operated at high temperature (above the melting temperature of PEO), the lack of doping in polymer LECs can be attributed to electrochemical side reactions involving the polymer electrolyte.[47] Such adverse side reactions, however, have not been observed in planar polymer LECs operated under high voltage and modest temperatures,[34−37] as was also the case in this study.

CONCLUSIONS

The LEC operating mechanism had been a subject of intense debate.[48,49] While the "electrodynamic" model attempts to explain the behaviors of LECs without invoking doping,[50] the results described above proved unambiguously that polymer LECs operate via in situ electrochemical doping and the formation of a light-emitting p−n junction. The elucidation of the p−n junction electronic structure, however, had just begun. This study showed that the p−n junction formed in an LEC is a graded p−n junction with a far more conductive p region than n region. Subsequent studies will focus on the determination of the absolute conductivities of the doped polymer films and the width of the depletion region. A p−n junction is ubiquitous in conventional semiconductor device applications. A better understanding of its polymer analogue is highly important, as it may lead to an entire class of molecular electronic devices that are based on high-performance homo- and heterojunctions.

ASSOCIATED CONTENT

Supporting Information. Experimental details. This material is available free of charge via the Internet at http://pubs.acs.org.

AUTHOR INFORMATION

Corresponding Author
jungao@physics.queensu.ca

ACKNOWLEDGMENT

This work is funded by the Natural Sciences and Engineering Research Council of Canada. The authors thank American Dye Source, Inc. for providing the MEH-PPV used in this work.

REFERENCES

(1) Heeger, A. J. *Chem. Soc. Rev.* **2010**, *39*, 2354.
(2) Friend, R. H.; Gymer, R. W.; Holmes, A. B.; Burroughes, J. H.; Marks, R. N.; Taliani, C.; Bradley, D. D. C.; Dos Santos, D. A.; Bredas, J. L.; Logdlund, M.; Salaneck, W. R. *Nature* **1999**, *397*, 121.
(3) Pivrikas, A.; Sariciftci, N. S.; Juska, G.; Osterbacka, R. *Prog. Photovoltaics* **2007**, *15*, 677.
(4) Kippelen, B.; Bredas, J. L. *Energy Environ. Sci.* **2009**, *2*, 251.
(5) Helgesen, M.; Sondergaard, R.; Krebs, F. C. *J. Mater. Chem.* **2010**, *20*, 36.
(6) Singh, T. B.; Sariciftci, N. S. *Annu. Rev. Mater. Res.* **2006**, *36*, 199.
(7) Facchetti, A. *Mater. Today* **2007**, *10*, 28.
(8) Gao, W. Y.; Kahn, A. *Org. Electron.* **2002**, *3*, 53.
(9) Tal, O.; Rosenwaks, Y.; Preezant, Y.; Tessler, N.; Chan, C. K.; Kahn, A. *Phys. Rev. Lett.* 2005, *95*, 256495-8.
(10) Kroger, M.; Hamwi, S.; Meyer, J.; Riedl, T.; Kowalsky, W.; Kahn, A. *Org. Electron.* **2009**, *10*, 932.
(11) Werner, A.; Li, F. H.; Harada, K.; Pfeiffer, M.; Fritz, L.; Leo, K.; Machill, S. *Adv. Funct. Mater.* **2004**, *14*, 255.
(12) Walzer, K.; Maennig, B.; Pfeiffer, M.; Leo, K. *Chem. Rev.* **2007**, *107*, 1233.
(13) Olthof, S.; Tress, W.; Meerheim, R.; Lussem, B.; Leo, K. *J. Appl. Phys.* 2009, *106*, 103711.
(14) Harada, K.; Werner, A. G.; Pfeiffer, M.; Bloom, C. J.; Elliott, C. M.; Leo, K. In *Organic Optoelectronics and Photonics*; Heremans, P. L. M. M. H. H., Ed.; SPIE: Bellingham, WA, 2004; Vol. 5464, p 1.
(15) Harada, K.; Werner, A. G.; Pfeiffer, M.; Bloom, C. J.; Elliott, C. M.; Leo, K. *Phys. Rev. Lett.* 2005, *94*, 036601.
(16) Tsuji, H.; Mitsui, C.; Sato, Y.; Nakamura, E. *Adv. Mater.* **2009**, *21*, 3776.
(17) Sivaramakrishnan, S.; Zhou, M.; Kumar, A. C.; Chen, Z. L.; Png, R. Q.; Chua, L. L.; Ho, P. K. H. *Appl. Phys. Lett.* 2009, *95*, 213303.
(18) Harada, K.; Riede, M.; Leo, K.; Hild, O. R.; Elliott, C. M. *Phys. Rev. B* 2008, *77*, 195212.
(19) Pei, Q. B.; Yu, G.; Zhang, C.; Yang, Y.; Heeger, A. J. *Science* **1995**, *269*, 1086.
(20) Pei, Q. B.; Yang, Y.; Yu, G.; Zhang, C.; Heeger, A. J. *J. Am. Chem. Soc.* **1996**, *118*, 3922.

(21) Sze, S. M. *Semiconductor Devices, Physics and Technology*; John Wiley & Sons: New York, 1985.
(22) Chiang, C. K.; Fincher, C. R.; Park, Y. W.; Heeger, A. J.; Shirakawa, H.; Louis, E. J.; Gau, S. C.; Macdiarmid, A. G. *Phys. Rev. Lett.* **1977**, *39*, 1098.
(23) Chiang, C. K.; Gau, S. C.; Fincher, C. R.; Park, Y. W.; Macdiarmid, A. G.; Heeger, A. J. *Appl. Phys. Lett.* **1978**, *33*, 18.
(24) Usuki, A.; Murase, M.; Kurauchi, T. *Synth. Met.* **1987**, *18*, 705.
(25) Koshida, N.; Wachi, Y. *Appl. Phys. Lett.* **1984**, *45*, 436.
(26) Wada, T.; Takeno, A.; Iwaki, M.; Sasabe, H.; Kobayashi, Y. *J. Chem. Soc.-Chem. Commun.* **1985**, 1194.
(27) Moliton, A.; Duroux, J. L.; Ratier, B.; Froyer, G. *Electron. Lett.* **1988**, *24*, 383.
(28) Cheng, C. H. W.; Lonergan, M. C. *J. Am. Chem. Soc.* **2004**, *126*, 10536.
(29) Leger, J. M.; Rodovsky, D. B.; Bartholomew, G. R. *Adv. Mater.* **2006**, *18*, 3130.
(30) Yu, Z. B.; Sun, M. L.; Pei, Q. B. *J. Phys. Chem. B* **2009**, *113*, 8481.
(31) Tang, S.; Irgum, K.; Edman, L. *Org. Electron.* **2010**, *11*, 1079.
(32) Gao, J.; Yu, G.; Heeger, A. J. *Appl. Phys. Lett.* **1997**, *71*, 1293.
(33) Gao, J.; Li, Y. F.; Yu, G.; Heeger, A. J. *J. Appl. Phys.* **1999**, *86*, 4594.
(34) Dane, J.; Tracy, C.; Gao, J. *Appl. Phys. Lett.* **2005**, *86*, 153509.
(35) Gao, J.; Dane, J. *Appl. Phys. Lett.* **2003**, *83*, 3027.
(36) Gao, J.; Dane, J. *Appl. Phys. Lett.* **2004**, *84*, 2778.
(37) Hu, Y.; Tracy, C.; Gao, J. *Appl. Phys. Lett.* **2006**, *88*, 123507.
(38) Shin, J. H.; Dzwilewski, A.; Iwasiewicz, A.; Xiao, S.; Fransson, A.; Ankah, G. N.; Edman, L. *Appl. Phys. Lett.* **2006**, *89*, 013509.
(39) Shin, J. H.; Edman, L. *J. Am. Chem. Soc.* **2006**, *128*, 15568.
(40) Pingree, L. S. C.; Rodovsky, D. B.; Coffey, D. C.; Bartholomew, G. P.; Ginger, D. S. *J. Am. Chem. Soc.* **2007**, *129*, 15903.
(41) Matyba, P.; Maturova, K.; Kemerink, M.; Robinson, N. D.; Edman, L. *Nat. Mater.* **2009**, *8*, 672.
(42) Hohertz, D.; Gao, J. *Adv. Mater.* **2008**, *20*, 3298.
(43) Hu, Y. F.; Gao, J. *Appl. Phys. Lett.* **2006**, *89*, 253514.
(44) Shin, J. H.; Matyba, P.; Robinson, N. D.; Edman, L. *Electrochim. Acta* **2007**, *52*, 6456.
(45) Rodovsky, D. B.; Reid, O. G.; Pingree, L. S. C.; Ginger, D. S. *ACS Nano* **2010**, *4*, 2673.
(46) Slinker, J. D.; DeFranco, J. A.; Jaquith, M. J.; Silveira, W. R.; Zhong, Y. W.; Moran-Mirabal, J. M.; Craighead, H. G.; Abruna, H. D.; Marohn, J. A.; Malliaras, G. G. *Nat. Mater.* **2007**, *6*, 894.
(47) Fang, J.; Matyba, P.; Robinson, N. D.; Edman, L. *J. Am. Chem. Soc.* **2008**, *130*, 4562.
(48) deMello, J. C. *Nat. Mater.* **2007**, *6*, 796.
(49) Pei, Q.; Heeger, A. J. *Nat. Mater.* **2008**, *7*, 167.
(50) deMello, J. C.; Tessler, N.; Graham, S. C.; Friend, R. H. *Phys. Rev. B* **1998**, *57*, 12951.